Springer Series on Atomic, Optical, and Plasma Physics 86

Markus Kitzler
Stefanie Gräfe *Editors*

Ultrafast Dynamics Driven by Intense Light Pulses

From Atoms to Solids, from Lasers to Intense X-rays

Springer

Springer Series on Atomic, Optical, and Plasma Physics

Volume 86

The Springer Series on Atomic, Optical, and Plasma Physics covers in a comprehensive manner theory and experiment in the entire field of atoms and molecules and their interaction with electromagnetic radiation. Books in the series provide a rich source of new ideas and techniques with wide applications in fields such as chemistry, materials science, astrophysics, surface science, plasma technology, advanced optics, aeronomy, and engineering. Laser physics is a particular connecting theme that has provided much of the continuing impetus for new developments in the field, such as quantum computation and Bose-Einstein condensation. The purpose of the series is to cover the gap between standard undergraduate textbooks and the research literature with emphasis on the fundamental ideas, methods, techniques, and results in the field.

More information about this series at http://www.springer.com/series/411

Markus Kitzler · Stefanie Gräfe
Editors

Ultrafast Dynamics Driven by Intense Light Pulses

From Atoms to Solids, from Lasers to Intense X-rays

Springer

Editors
Markus Kitzler
Photonics Institute
Vienna University of Technology
Vienna
Austria

Stefanie Gräfe
Institute for Physical Chemistry
University of Jena
Jena
Germany

ISSN 1615-5653 ISSN 2197-6791 (electronic)
Springer Series on Atomic, Optical, and Plasma Physics
ISBN 978-3-319-20172-6 ISBN 978-3-319-20173-3 (eBook)
DOI 10.1007/978-3-319-20173-3

Library of Congress Control Number: 2015943437

Springer Cham Heidelberg New York Dordrecht London

Printed on acid-free paper

Springer International Publishing AG Switzerland is part of Springer Science+Business Media (www.springer.com)

Preface

The properties of matter are ultimately determined by its electronic structure. A suitable perturbation of the electrons' distribution from its equilibrium configuration in a system such as an atom, a molecule, or a solid, can therefore initiate certain dynamical processes. Intense and ultrashort light pulses are ideal tools for that purpose as their electric fields couple directly to the electrons. Therefore, they are not only able to distort the equilibrium electron distribution but, even allow driving a system on sub-femtosecond timescales with the light's Petahertz field-oscillations. This has been realized first in experiments that studied atoms in strong laser fields some 25 years ago. These experiments revealed a wealth of fundamentally important phenomena that are strictly timed to the laser-field oscillations such as the release of electrons by tunneling through the field-distorted Coulomb binding potential, or field-driven (re-)collisions of the released electrons with the atomic ion. The latter, in turn, led to the discovery of a range of essential secondary processes such as the generation of very high orders of harmonics of the driving light with photon energies that can extend into the X-ray range.

Since then, thanks to a true revolution in laser technology, tremendous progress has been made in the field. Laser science has now reached a level of perfection where it is possible to produce intense light pulses with durations down to a single oscillation cycle and with virtually arbitrary evolution of the electric field in a wide range of frequencies. The availability of such field transients enabled a number of exciting possibilities, such as control over the breakage of selected chemical bonds in molecules by directly driving the molecular valence electrons that actually form the bond, or the production of coherent attosecond pulses in the soft X-ray wavelength range that can be used for probing or initiating dynamics on time-intervals during which the electronic distribution in the system under study stays essentially frozen.

The recent years have seen a particularly vivid progress in the research of using ultrashort intense light pulses for controlling and probing ultrafast dynamics. On the one hand, a number of groups have extended the research field to systems with a much increased complexity and have studied and controlled field-induced dynamics in large polyatomic molecules, cluster complexes, bio-matter, nanoparticles and crystals, and also in condensed phase systems such as solid surfaces,

nanostructures, and bulk solids. On the other hand, the availability of new, coherent light sources in both the very short (X-rays) and very long (mid-infrared) wavelength ranges have allowed for the production and application of short and intense pulses in previously unexplored regimes.

Owing to this large diversity of pulsed sources and dynamical systems studied with them it becomes inherently difficult to provide a unique definition and sharp boundaries for this field of research. This is also reflected by the considerable variety of titles used for conferences in this field. Obviously the same difficulty arises in providing a clear and well-defined but at the same time comprehensive title for a book on this research field. Although *ultrafast dynamics* is a relative term and covers a large range of dynamical processes and timescales, including rotational and vibrational dynamics, we would like to define this term here as electronic dynamics and processes that result from an essentially instantaneous distortion of the equilibrium electronic structure in a given system.

With this book we have tried, by carefully picking 14 examples of cutting-edge scientific research, grouped in four areas, to provide a comprehensive overview not only over the current state of the research field that uses ultrashort intense light pulses and light sources based on these pulses for initiating, driving, controlling, and probing ultrafast dynamics, but also over its recent tremendous and exciting developments. With the selection of the four areas we have attempted to provide the broadest possible overview over the such defined research field by covering essentially all currently studied physical systems from individual atoms and molecules to nanostructures and bulk macroscopic media, and all available ultrafast pulse sources from the mid-infrared to the X-ray range. Of particular importance for us was to highlight the possibilities that are opened up by the availability of new light sources, and the new research questions that arise by pushing research toward new systems with increased complexity such as nanostructures and bulk macroscopic media. Also, we have tried to provide both an experimental and theoretical perspective on the research field. The book is structured as follows.

The first part of research that is discussed during the first four chapters shall provide an overview of the possibilities that a strong laser field opens up for controlling electronic processes in atoms, molecules, nanostructures, and solids. *The second part* of the book is dedicated to the application of intense laser pulses in combination with attosecond pulses, obtained by the laser-driven process of high-harmonic generation, for triggering and probing ultrafast dynamics. *The third part* of the book discusses in four chapters the only very recently opened research route of using ultrashort intense laser pulses for driving electronic dynamics on surfaces, in nanostructures and in solids. While on the one hand this type of research is interesting from a fundamental point of view as it investigates the interaction of light and matter in completely new regimes of parameters where collective effects, material parameters, and system geometries start to play a role, this research also comprises considerable potential for applications in that it could be used for, e.g., fabrication of devices for information transmission or fast switching. A particularly important process in this context is the excitation of collective surface electron oscillations called a surface plasmon. *The fourth and*

final part of the book is dedicated to the exciting possibilities that are opened up by the availability of intense light pulses in the X-ray wavelength regime that can be produced by free-electron lasers, the first of which have started their operation just a few years ago. The two chapters in this part discuss applications of such pulses depicted by examples of research performed at the free-electron lasers in Hamburg (FLASH) and Stanford (Linac Coherent Light Source, LCLS), respectively.

We hope that this book will be equally inspiring and helpful for young researchers, who would like to step into this field, and for experienced researchers who may enjoy the exhaustive discussion that covers the research on essentially all currently studied objects and with all available ultrafast pulse sources in the field that uses ultrashort light pulses for controlling and probing ultrafast dynamics.

Vienna — Markus Kitzler
Jena — Stefanie Gräfe

Contents

Contributors

Jakob Andreasson Molecular Biophysics Department of Cell and Molecular Biology (ICM), Uppsala University, Uppsala, Sweden; ELI-Beamlines, Institute of Physics, Academy of Sciences of the Czech Republic, Prague, Czech Republic

Thomas Barillot Institut Lumière Matière ILM, CNRS, Villeurbanne CEDEX, France

Thomas Baumert Universität Kassel, Institut für Physik und CINSaT, Kassel, Germany

Tim Bayer Carl von Ossietzky Universität Oldenburg, Institut für Physik, Oldenburg, Germany

Jérémie Caillat UPMC, UMR 7614, Laboratoire de Chimie Physique—Matière et Rayonnement 11, Paris Cedex 05, France; CNRS, UMR 7614, Laboratoire de Chimie Physique—Matière et Rayonnement 11, Paris Cedex 05, France

Francesca Calegari Institute of Photonics and Nanotechnologies, IFN-CNR, Milano, Italy

J. Marcus Dahlström Department of Physics, Stockholm University, AlbaNova University Center, Stockholm, Sweden; Max-Planck Institute for the Physics of Complex Systems, Dresden, Germany

Victor Despré Institut Lumière Matière ILM, CNRS, Villeurbanne CEDEX, France

Péter Dombi MTA "Lendület" Ultrafast Nanooptics Group, Wigner Research Centre for Physics, Budapest, Hungary

Reinhard Dörner Institut Für Kernphysik, Goethe Universität, Frankfurt, Germany

K.E. Echternkamp IV. Physical Institute—Solids and Nanostructures, University of Göttingen, Göttingen, Germany

U. Eichmann Max-Born-Institute, Berlin, Germany

Jason Greenwood Centre for Plasma Physics, School of Maths and Physics, Queen's University Belfast, BT7 1NN, UK

Markus Gühr PULSE, SLAC National Accelerator Laboratory and Stanford University, Menlo Park, CA, USA

Stefan Haessler Photonics Institute, Vienna University of Technology, Vienna, Austria; LOA, ENSTA ParisTech, CNRS, Ecole Polytechnique, Université Paris-Saclay, Palaiseau Cedex, France

G. Herink IV. Physical Institute—Solids and Nanostructures, University of Göttingen, Göttingen, Germany

Ferenc Krausz Max-Planck-Institut für Quantenoptik, Hans-Kopfermann-Straße 1, Garching, Germany; Ludwig-Maximilians-Universität, Am Coulombwall 1, Garching, Germany

Maria Krikunova Institut Für Optik und Atomare Physik, Technische Universität Berlin, Berlin, Germany

Stanislav Yu. Kruchinin Max-Planck-Institut für Quantenoptik, Hans-Kopfermann-Straße 1, Garching, Germany

Franck Lépine Institut Lumière Matière ILM, CNRS, Villeurbanne CEDEX, France

Candong Liu State Key Laboratory of High Field Laser Physics, Shanghai Institute of Optics and Fine Mechanics, Chinese Academy of Sciences, Shanghai, China

Vincent Loriot Institut Lumière Matière ILM, CNRS, Villeurbanne CEDEX, France

Matteo Lucchini Department of Physics, ETH Zurich, Zürich, Switzerland

Mattia Lupetti Ludwig Maximilians Universität, Munich, Germany

Alfred Maquet UPMC, UMR 7614, Laboratoire de Chimie Physique—Matière et Rayonnement 11, Paris Cedex 05, France; CNRS, UMR 7614, Laboratoire de Chimie Physique—Matière et Rayonnement 11, Paris Cedex 05, France

Alexandre Marciniak Institut Lumière Matière ILM, CNRS, Villeurbanne CEDEX, France

Dejan B. Milošević Faculty of Science, University of Sarajevo, Sarajevo, Bosnia and Hercegovina; Academy of Sciences and Arts of Bosnia and Hercegovina, Sarajevo, Bosnia and Hercegovina; Max-Born-Institut, Berlin, Germany

Mauro Nisoli Institute of Photonics and Nanotechnologies, IFN-CNR, Milano, Italy; Department of Physics, Politecnico di Milano, Milano, Italy

Tim Paasch-Colberg Max-Planck-Institut für Quantenoptik, Hans-Kopfermann-Straße 1, Garching, Germany

Maurizio Reduzzi Department of Physics, Politecnico di Milano, Milano, Italy

C. Ropers IV. Physical Institute—Solids and Nanostructures, University of Göttingen, Göttingen, Germany

Arnaud Rouzée Max-Born Institute (MBI), Berlin, Germany

Giuseppe Sansone Institute of Photonics and Nanotechnologies, IFN-CNR, Milano, Italy; Department of Physics, Politecnico di Milano, Milano, Italy

Armin Scrinzi Ludwig Maximilians Universität, Munich, Germany

M. Sivis IV. Physical Institute—Solids and Nanostructures, University of Göttingen, Göttingen, Germany

Mark I. Stockman Center for Nano-Optics (CeNO) and Department of Physics and Astronomy, Georgia State University (GSU), Atlanta, GA, USA

Nicusor Timneanu Molecular Biophysics Department of Cell and Molecular Biology (ICM), Uppsala University, Uppsala, Sweden; Department of Physics and Astronomy, Uppsala University, Uppsala, Sweden

Xiao-Min Tong Division of Materials Science, Faculty of Pure and Applied Sciences, University of Tsukuba, Tsukuba, Ibaraki, Japan; Center for Computational Sciences, University of Tsukuba, Tsukuba, Ibaraki, Japan

Nobuyuki Toshima Division of Materials Science, Faculty of Pure and Applied Sciences, University of Tsukuba, Tsukuba, Ibaraki, Japan

Andrea Trabattoni Department of Physics, Politecnico di Milano, Milano, Italy

Morgane Vacher Department of Chemistry, Imperial College London, London, United Kingdom

Marc. J.J. Vrakking Max-Born Institute (MBI), Berlin, Germany

L. Wimmer IV. Physical Institute—Solids and Nanostructures, University of Göttingen, Göttingen, Germany

Matthias Wollenhaupt Carl von Ossietzky Universität Oldenburg, Institut für Physik, Oldenburg, Germany

Jian Wu State Key Laboratory of Precision Spectroscopy, East China Normal University, Shanghai, China

Vladislav S. Yakovlev Max-Planck-Institut für Quantenoptik, Hans-Kopfermann-Straße 1, Garching, Germany; Ludwig-Maximilians-Universität, Am Coulombwall 1, Garching, Germany

S.V. Yalunin IV. Physical Institute—Solids and Nanostructures, University of Göttingen, Göttingen, Germany

Part I
Control of Electronic Processes with Strong Laser Fields

Chapter 1
Strong-Field Induced Atomic Excitation and Kinematics

U. Eichmann

Abstract Frustrated tunneling ionization (FTI) has recently been found to be an important exit channel of atomic strong-field ionization models such as the simple man's or rescattering model if one considers the Coulomb field explicitly. It leads to the population of bound excited states rather than to ionization after the electron has tunneled and quivered in the laser field. In this chapter we introduce the FTI model and describe experiments whose outcome supports its importance. In particular, we focus on strong-field excitation of atoms and the observation of neutral (ionic) excited fragments with high kinetic energy in strong-field fragmentation and Coulomb explosion of small molecules. Furthermore, we present experiments in which a direct position sensitive detection of excited neutral atoms reveals the exceptionally high acceleration of atoms in short pulsed strongly focused laser fields and discuss possible applications.

1.1 Introduction

The understanding of strong-field ionization dynamics of atoms and molecules rests a great deal on the seminal tunneling picture introduced by Keldysh [1]. A linearly polarized pulsed strong laser field is considered as a classical electric field $\mathbf{F}(t) = \mathbf{F}_L(t)\cos(\omega t)$ with $\mathbf{F}_L(t) = f(t)F_0\hat{\mathbf{e}}_\mathbf{x}$, where $f(t)$ is a slowly time-varying pulse envelope, F_0 is the field amplitude and ω is the angular frequency of the laser. All equations throughout the paper are given in atomic units unless otherwise stated. If an atom in its ground state with an ionization potential I_P is exposed to such a laser field, the atomic Coulomb potential is periodically bent up and down and allows for tunneling of an electron at certain phases of the laser field. The pure tunneling picture describes ionization extremely well, particularly in those situations, where a fairly large number of photons is necessary to overcome the binding energy. The Keldysh parameter $\gamma = \sqrt{I_P/2U_p}$, where $U_p = F^2/4\omega^2$ is the ponderomotive potential, is

U. Eichmann (✉)
Max-Born-Institute, Max-Born-Strasse 2a,12489 Berlin, Germany
e-mail: eichmann@mbi-berlin.de

M. Kitzler and S. Gräfe (eds.), *Ultrafast Dynamics Driven by Intense Light Pulses*, Springer Series on Atomic, Optical, and Plasma Physics 86, DOI 10.1007/978-3-319-20173-3_1

used to distinguish the tunneling regime $\gamma < 1$ from the multiphoton regime $\gamma > 1$. It has been found, however, that the subsequent dynamics of the electron in the laser field is of decisive importance. It results in secondary processes, which are embraced in the simple man's model [2–4] and in the famous three-step or rescattering model [5–7]. The simple man's model concentrates on the cycle-averaged energy a liberated electron can extract from the classical laser field, neglecting any interaction with the parent ion in the first place. The rescattering model, on the other hand, focuses on the processes initiated after the first return(s) of the electron to the core, where particularly electrons liberated in a certain phase range after a field cycle maximum provide high kinetic energies at the return. These processes include high-order above threshold ionization (HATI) [8], non-sequential double or non-sequential multiple-ionization (NSDI) by collision [9–12] and radiative recombination generating high harmonics (HHG) [13, 14].

We will concentrate on the dynamics of electrons, which tunnel around the field cycle maximum thus avoiding substantial energy transfer during rescattering with the parent ion. Astonishingly, the physical consequences that arise in the context of these electrons have not been considered coherently before, neither in the simple man's model nor in the rescattering model. By taking into account the Coulomb field explicitly, one finds that ionization of the atom, expected to follow the tunneling process of the electron, is frustrated under certain circumstances. This exit channel leads to the population of excited states. The process, which has been dubbed frustrated tunneling ionization (FTI), describes quantitatively (quasi multi-photon) excitation within the tunneling picture [15].

To put the FTI model into perspective one has to mention that since the early days of optical strong-field physics, experiments have shown beside multiphoton ionization also multiphoton excitation [16–19]. In the multiphoton picture, it was argued qualitatively that a Rydberg state is excited at the beginning of the laser pulse. Similar to a free electron the quasi free Rydberg electron does not absorb energy from the electromagnetic field and remains bound. The picture of Rydberg state excitation was strongly supported by the observation of strong enhancements in the above threshold ionization (ATI) electron spectra, which were explained in terms of transient Freeman resonances [20]. These are Rydberg states that are shifted ponderomotively into resonance with the laser field at particularly intensities during the rise of the laser pulse and subsequently ionized. To explain why an atom in a Rydberg state is finally stable against ionization, different stabilization mechanisms [21] such as interference stabilization at lower intensities [22–27] or strongly reduced ionization rates due to high angular momentum [17, 28] have been suggested. An easy quantitative explanation of excitation in the multiphoton picture, however, has not been achieved.

We remark that population trapping in excited states should not be misinterpreted with atomic stabilization in strong laser fields. Simply speaking the strong-field actually stabilizes the atom by reducing the overlap of the laser driven electronic wave function with the ionic core. This phenomenon, usually associated with the situation that a single-photon absorption is in principle sufficient to ionize, was first predicted about a quarter century ago [29–32]. Since then, the subject has been extensively

discussed theoretically for the last two decades [33, 34] with newly increased interest [35, 36]. Stabilization of a single prepared low lying Rydberg state in a moderately strong laser field without any remaining loop holes such as state redistribution has been observed in impressive experiments [37, 38].

The qualitative arguments expressed within the multiphoton picture were also applied to explain excitation of atoms in the strong-field tunneling regime. In [18, 39] high-lying Rydberg states after strong-field interaction were observed by subsequent field ionization and in [40], e.g., excitation was deduced from structures in the measured ionization yields. First trials to explain excitation in the strong-field tunneling regime have been given within the simple man's model [2–4]. Early investigations on stabilization of atoms using classical Monte Carlo analysis [41] found as an alternate way to stabilization that the quivering electrons land on Rydberg states after the laser pulse has terminated. Yudin and Ivanov reported transient Rydberg trajectories [42] in the tunneling regime and finally Muller concluded from extensive quantum mechanical calculation excitation in the tunneling regime [43]. Only recently excited states of He have been observed [15], in which the intensities were well in the tunneling regime of strong-field physics. The obvious question that arose in this context was whether there is a way to comprehend strong-field excitation purely within the tunneling picture without invoking the multiphoton picture. The solution lies in the frustrated tunneling ionization model, which describes astonishingly well observed features.

In the following sections we will elucidate in detail how frustrated tunneling ionization leads to excited states and we will discuss consequences for strong-field physics. Besides important ramifications in atomic strong-field physics we also find FTI at work in strong-field dissociation of molecules. Finally, FTI establishes the basis to explain observed kinematic effects of strong inhomogeneous fields on neutral atoms.

1.2 Strong Field Excitation of Atoms by Frustrated Tunneling Ionization (FTI)

1.2.1 Linearly Polarized Laser Fields

In tunneling models, the tunneling process is mostly regarded to be tantamount to tunneling ionization. This is correct, if no attractive potential, whatsoever, is explicitly considered in the first place. However, by taking into account the Coulomb potential of the parent ion, frustrated tunneling ionization might happen. Assuming that the tunneling process is instantaneous at some time t_t, the electron is then located at the tunnel exit, which is only a few Bohr radii away from the ionic core. At this point, the electron has a high negative potential energy of a few eV. The electron quivers in the strong laser field and, whenever the tunneled electron does not gain enough energy during the interaction with both the laser field and the Coulomb field to finally

overcome the attractive Coulomb force [15], it has not been set free at all. Therefore, one expects FTI to occur mainly for electrons that tunnel in the vicinity of a field cycle maximum of a linearly polarized laser field at a phase $\phi_t = \omega t_t \approx 0$ (or a multiple integer of π). In this case, the laser induced drift energy, given by $E_{dr} = 2U_p \sin^2 \phi_t$ [19], is close to zero and also the energy upon the first rescattering on the parent ion is rather moderate and typically less than the potential energy in the Coulomb field.

Decisive, whether ionization occurs after tunneling, or not, is the total energy T of the electron at a time, when the laser pulse is over. If it is positive, the electron motion is eventually unbound, if it is negative, the electron will firmly relax into a bound state. Again, the notion in the rescattering model that the "electron tunnel ionizes in the first step" is correct as long as no attractive potential is considered. In the presence of an attractive potential one can assert that ionization has happened only after the laser pulse is over . Consequently, thinking in terms of the rescattering model, where it is common agreement that an electron is considered to be "ionized" after the tunneling process, the term frustrated tunneling ionization is meaningful and justified. However, it is most important to emphasize that an electron that has undergone frustrated tunneling ionization, has in fact never been unbound in the sense of a strict definition of ionization.

In the following we will explore the parameter range for producing bound excited states through FTI. For given laser pulse parameters and a specified atom, which will be Helium in the present examples, the position and momentum of the electron, and the phase ϕ_t of the oscillating laser field at the instant of tunneling are crucial [15, 44]. To calculate trajectories leading to frustrated tunneling ionization we solve the classical Newton equations for an electron in a combined pure Coulomb potential $V_c(r) = -1/r$, where $r = \sqrt{x^2 + y^2 + z^2}$, and the electric field $\mathbf{F}(t)$.

$$\ddot{\mathbf{x}}(\mathbf{t}) = -\mathbf{F}(t) - \nabla V_c(r(t)) \tag{1.1}$$

The initial conditions at t_t are obtained from the tunneling ionization model, which locate the tunneling exit in a linearly polarized laser field at $x(t_t) = -\left(I_P + [I_P^2 - 4\,|F(t_t)|]^{1/2}\right)/2F(t_t)$, and $y(t_t) = z(t_t) = 0$. Furthermore, at t_t, the longitudinal momentum of the electron along the polarization axis is $p_x(t_t) = 0$. The initial momentum perpendicular to the field axis $p_\perp(t_t) = \sqrt{p_y^2 + p_z^2}$ is a parameter. To get an overview over bound and unbound trajectories we exploit the fact that trajectories are planar and symmetric with respect to the field axis. We thus vary p_y and take $p_z = 0$.

In Fig. 1.1 we show the occurrence of bound trajectories as a function of the parameters $\phi_t = \omega t_t$ and p_y. For clarity we restrict the electron to tunnel only in the vicinity of the field cycle maximum at the laser pulse envelope maximum. The calculations are performed with a linearly polarized laser pulse with 8 fs (FWHM) pulse duration and field strengths of $F_0 = 0.0755$ a.u. and $F_0 = 0.169$ a.u., Fig. 1.1a, b, respectively, and with 29 fs (FWHM) pulse duration and the same field strengths as before, Fig. 1.1c, d, respectively. The Keldysh parameters associated with the two field strengths are $\gamma = 1$ and $\gamma = 0.44$, respectively. Obviously, there are only

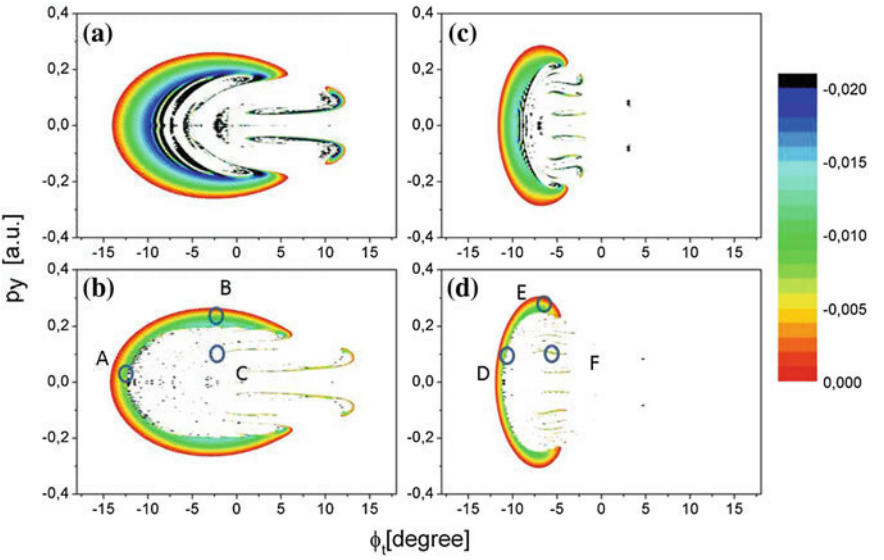

Fig. 1.1 Occurence of bound states after tunneling. Laser parameters: $F_0 = 0.0755$ a.u. (2×10^{14} W cm^{-2}) and **a** 8 fs (FWHM) and **b** 29 fs (FWHM) pulse duration. Laser parameters: $F_0 = 0.169$ a.u. (10^{15} W cm^{-2}) and **c** 8 fs and **d** 29 fs pulse duration. The *circles* indicate initial parameters for calculated trajectories shown in Fig. 1.2. The phase $\phi_t = \omega t_t$ is indicated with respect to the field cycle maximum at the maximum of the laser pulse envelope. Final negative total energy T of the electron is color coded. *White areas* stand for trajectories with positive total energy corresponding to strong-field ionization

certain well defined regions of the parameters, where frustrated tunneling ionization prevails. Inspecting Fig. 1.1a, b one finds that the parameter space for bound trajectories is much larger for electrons starting before the maximum than for electrons starting after it. Particularly, for the short laser pulses, Fig. 1.1a, one finds a relatively large region of parameters allowing for bound states [44]. In this case the laser drift momentum the electron acquires is opposite to the Coulomb force. If the electron starts after the field cycle maximum, the recollision with the ionic core is likely, which obviously counteracts formation of bound states. At longer pulse duration, Fig. 1.1b, on the other hand, the allowed parameter range is reduced and is characterized by distinct isolated areas. Apparently, bound states are no longer populated due to the higher probability of a fatal encounter of the electron with the ionic core at longer pulse durations. If we increase the field amplitude and use otherwise identical laser parameters, the parameter space for bound trajectories shrinks substantially, Fig. 1.1c, d. Most striking is that bound states are no longer found for electrons that tunnel after the field cycle maximum.

The interesting question that arises is how important is the influence of the Coulomb potential on the electron dynamics during the laser pulse? It is well known that most of the strong-field physics associated with the rescattering model

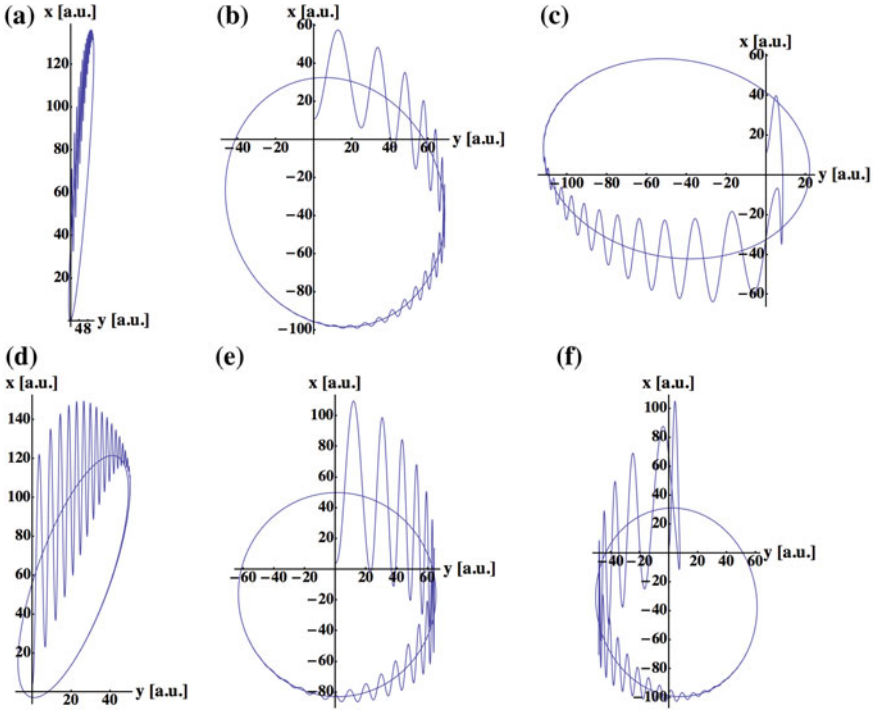

Fig. 1.2 Selected trajectories for initial conditions indicated in Fig. 1.1

is well described without invoking the Coulomb potential. To shed more light on the dynamics, it is very instructive to visualize and study electron trajectories at specific (ϕ_t, p_y) parameters. We show different trajectories along an energy contour line with $E_b \approx -7.8 \times 10^{-3}$ a.u. corresponding to roughly a principal quantum number $n = 8$. The initial conditions for trajectories shown in Fig. 1.2a–c are indicated in Fig. 1.1b by A–C, resp., and the initial conditions for trajectories shown in Fig. 1.2d–f are indicated in Fig. 1.1d by D–F, resp. The trajectories are calculated for several revolutions, so that the wiggly motion at early times during the laser pulse superimposes the final bound orbit at later times.

Trajectories, shown in (a) and (d), and in (b) and (e), were calculated using similar initial conditions, respectively. However, the quiver amplitude has more than doubled in (b) and (d), as expected for the higher field strength. In (a) and (c) the final bound orbits are oriented along the laser polarization with low angular momentum owing to the low initial perpendicular momentum. The role of the Coulomb field is important and by no means negligible, since the maximum excursion of the electron after the laser pulse is smaller than expected on the basis of a Coulomb field free motion. The same is true for the orbits shown in Fig. 1.2b, e. Here, the drift motion solely due to the laser field is weak, so that the electron is dominantly under the influence of the strong Coulomb field. Furthermore, the quiver motion averaged over one

laser period follows astonishingly well the final Coulomb orbit almost right from the start indicating that the Coulomb potential plays a significant role at each stage of the orbit. In Fig. 1.2c we show a trajectory, where the tunneling process started after the field cycle maximum so that the laser drift momentum pushes the electron initially towards the core. It is obvious that in this case the average over the wiggly trajectory at short times does not follow the orbital motion, but due to the close encounter with the ionic core the electron uses a complicated shortcut at some point, before it behaves regularly again. Overall, the bound orbits on an isoenergy shell behave regularly. They show a decrease of the eccentricity e of the orbit equivalent to an increase in angular momentum l, with increasing initial lateral momentum. Orbits calculated with parameters of isolated areas in the parameter space around the field cycle maximum show initially strongly irregular behavior. The occurrence of bound trajectories with initial parameters taken from the inner parameter space region strongly depends on the number of laser cycles following the tunneling event, as the electron dynamics is dominated by strong rescattering at the core. This is reflected in irregular behavior during the laser pulse, before the orbit finally merges into a stable orbit, as can be seen in Fig. 1.2f.

To summarize the semiclassical analysis, we conclude that the population of bound excited states stems from an interplay of the Coulomb field and the laser field on equal footing. Often, the averaged motion of the electron during the laser pulse follows already nicely the trajectory of the final orbit it will merge into. Consequently, any approximation of the Coulomb interaction during the laser field is not a priori justified. Although the Coulomb field influences the overall trajectory decisively, the amplitude of the electron's quiver motion seems to be still in accord with the assumption of a quasi free electron quivering in the laser field.

To calculate the yield of excited states one has to consider the probability for tunneling of an electron in the ground state with the magnetic quantum number $m = 0$, which is given within the simplest approximation of the tunneling model by [42, 45, 46]

$$w_0 \propto \left(\frac{2(2I_P)^{3/2}}{|F(t_t)|}\right)^{\left(\frac{2}{\sqrt{2I_P}}-1\right)} \exp\left[-2(2I_P)^{3/2}/3\,|F(t_t)|\right]. \tag{1.2}$$

The probability to find a certain lateral momentum is given by [45]

$$w_\perp \propto \exp\left[-p_\perp^2\sqrt{2I_P}/\,|F(t_t)|\right]. \tag{1.3}$$

In semiclassical Monte-Carlo simulations one uses (1.2) and (1.3) to randomly pick initial conditions and start typically about 10^5–10^6 trajectories. The total energy $T = p(t_{fin})^2/2 + V(r(t_{fin}))$ of each trajectory is evaluated at time t_{fin} shortly after the laser pulse is over. As an example, we evaluate trajectories for He exposed to a laser field with intensities between (10^{14} and 10^{15} W cm^{-2}) and a laser pulse duration ($\tau = 27$ fs). We find $\approx$10 % of all launched trajectories to be bound at the lower

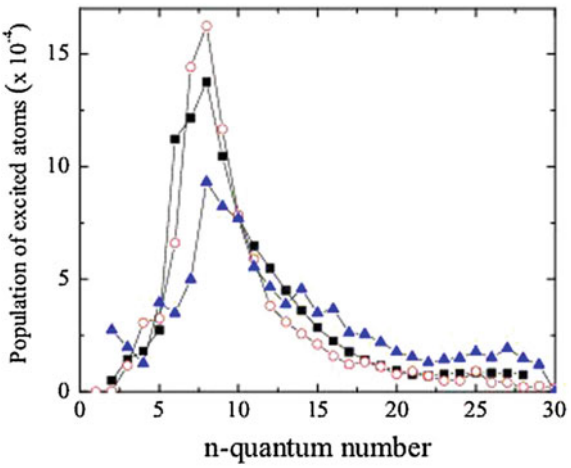

Fig. 1.3 n distribution of the population of excited states from a MC simulation (*red circle*), a quasi-one-electron (*black square*) and a full two-electron quantum mechanical calculation (*blue triangle*) at a laser intensity 10^{15} W cm^{-2}. The MC simulation has been normalized to the quasi-one-electron calculation at $n = 10$. From [15]

intensity 10^{14} W cm^{-2} and $\approx$2.5 % at 10^{15} W cm^{-2}, see Fig. 1 of [15], confirming the FTI process to be an important exit channel.

One can then assign an effective quantum number ν to each trajectory with negative total energy, determined by the Rydberg formula $T = -1/2\nu^2$. By sorting the effective quantum numbers into integer bins one obtains an n distribution, as shown in Fig. 1.3 and which is taken from [15]. The maximum of the distribution is around $n = 8$ and the probability drops steeply towards both sides, but allowing for Rydberg states with higher n quantum numbers. An analysis of the classical angular momentum reveals that for states with $n < 9$, the probability to find a specific angular momentum within a fixed n shell increases strongly towards the maximum allowed value of $l = n - 1$. For larger n states, we find the same distribution with no angular momentum states higher than $l = 9$.

It is also instructive to look at the wavelength dependence of the yield of bound states. The drift energy and the quiver amplitude both scale $\propto \omega^{-2}$ at constant laser intensity. Consequently, for shorter wavelengths the range of the parameter space for bound states increases and, with it, also the number of surviving trajectories. Particularly, population of lower n states with low radial extension benefits from the reduced quiver amplitude. On the other hand, increasing the wavelength results in the opposite behavior. Due to higher drift energy and a larger quiver motion, the parameter space for allowed trajectories shrinks and only bound trajectories with sufficient radial extension survive. The number of atoms surviving in lower n states is strongly diminished, while the number of atoms in higher n states remains the same. Consequently, the percentage of surviving atoms decreases. Finally, we mention that the FTI mechanism should also be in effect for strong-field excitation of ionic systems, see also Sect. 1.3.3.

The distribution shown in Fig. 1.3 has been confirmed by Monte-Carlo simulations of other groups [44, 47]. Most astounding, however, is the outcome of a direct comparison of the FTI results with TDSE calculations. In [15] the classical pre-

dictions were compared with results using the single-active electron (SAE) model and a full two-electron calculation, performed in the group of A. Saenz. The composition of the resulting Rydberg wave packet is in striking agreement, Fig. 1.3. The results demonstrate the predictive power of the frustrated tunneling ionization model. Similar results for the n distribution for different atoms and conditions have been obtained from other TDSE calculations [48–51] showing a maximum in the vicinity of $n = 8$. Only recently, we succeeded in measuring the n distribution by using a state selective field ionization method on the surviving neutral excited atoms. The results nicely confirm the theoretical predictions [52].

1.2.2 Elliptically Polarized Laser Fields

So far, we have described the FTI process in linearly polarized laser light. Hereby, most electrons tunnel in the vicinity of the field cycle maximum, so that the associated laser induced drift energy $E_{dr} \approx 0$. In an elliptically polarized laser field given by

$$\mathbf{F}(t) = F_0 f(t) \left(\cos(\omega t)\hat{\mathbf{e}}_x + \epsilon \sin(\omega t)\hat{\mathbf{e}}_y\right)/\sqrt{1+\epsilon^2}, \tag{1.4}$$

however, an additional laser induced drift momentum in y direction (lateral direction) arises, which reads for $\phi_t \approx 0$ $p_{dr,y} = -\epsilon F_0/\omega\sqrt{\epsilon^2+1}$. $p_{dr,y}$, and thus the total drift energy, are always nonzero for electrons that tunnel at $\phi_t \approx 0$ and increase strongly with ellipticity ϵ. It is this strong drift momentum that reduces substantially the population of bound states in elliptically polarized light. To include the polarization dependence, one might require in a simple approach that $p_{dr,y}$ must be compensated by an appropriate initial lateral momentum, $p_\perp = -p_{dr,y}$ to obtain bound states. Inserting this into (1.3), $w(\epsilon)$ is then given by [53]

$$w(\epsilon) \approx \exp -\frac{F_0(2I_p)^{1/2}}{\omega^2}\epsilon^2. \tag{1.5}$$

The results of this equation are in very good agreement with the experiment [15], which measured the total excited neutral yield as a function of ellipticity as shown in Fig. 1.4. We note that more extensive results have been obtained [47, 53] by solving (1.1) with the elliptically polarized laser field (1.4).

1.2.3 Intermediate Conclusion

The systematic investigation of electron trajectories emerging in a time window around a field cycle maximum revealed that the explicit inclusion of the Coulomb field in the rescattering model or simple man's model leads to bound states. Although bound or transient bound electron trajectories have been displayed occasionally in

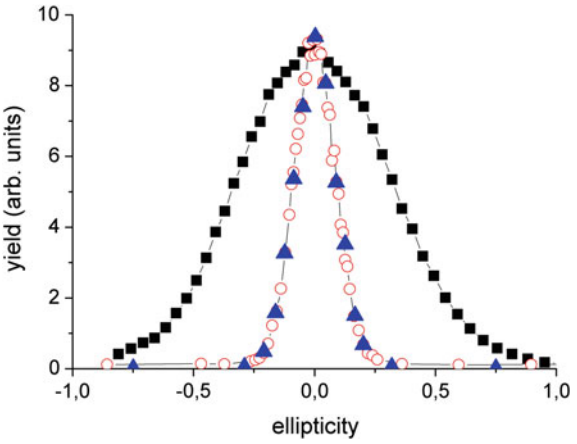

Fig. 1.4 Dependence of the He^+ (*black square*) and He^* (*red circle*) yield on the ellipticity at fixed laser intensity of 10^{15} W cm^{-2}. For better comparison the height of both measurements have been set equal at $\epsilon = 0$, from [15]. Theoretical data points (*blue triangle*) are taken from [53]

the literature, the systematic study has shaped a clear picture of excitation in the tunneling regime. The FTI model also facilitates the interpretation of more complex experiments involving bound states and has led to a simple way to make quantitative predictions, in particular on the total yield of bound states and their n distribution. The FTI process shows qualitatively a similar behavior on ellipticity as the rescattering related processes HHG, NSDI, and HATI. In the latter cases, however, elliptical polarization reduces the rescattering probability with the ionic core, while in the FTI process formation of bound states is suppressed due to the high drift momentum. Nevertheless, one can consider the FTI process as a relevant additional exit channel in the rescattering model. It is important to note that if one uses the correct definition of the term ionization, which has no strict meaning unless the laser pulse is off, an atom finally in a bound excited state has never become ionized in the first place. This, in turn, implies that the process is not a classical electron recombination process involving emission of radiation as has been misleadingly argued occasionally in the literature [49, 50].

1.2.4 Detection of Excited Atoms

The most prominent detection schemes in strong-field physics involve electron and ion detection by means of time of flight (TOF) techniques, velocity map imaging (VMI) [54], or a reaction microscope [55], as well as detection of high harmonic radiation. Usually, excited states of an atom are detected by subsequent photoionization or state selective field ionization, occasionally also by fluorescence measurements. In the scope of the present investigations experiments are based on a direct measurement. In Fig. 1.5 the sketch of an experimental setup shows how it is realized.

A well collimated thermal effusive beam of atoms, which is directed towards a position-sensitive multichannel plate (MCP) detector, is crossed by an intense